

This item is the archived peer-reviewed author-version of:

In vitro Phase I and Phase II metabolism of alpha-pyrrolidinovalerophenone (alpha-PVP), methylenedioxyprovalerone (MDPV) and methedrone by human liver microsomes and human liver cytosol

Reference:

Negreira Ferrol Noelia, Erratico Claudio, Kosjek Tina, van Nuijs Alexander, Heath Ester, Neels Hugo, Covaci Adrian.- In vitro Phase I and Phase II metabolism of alpha-pyrrolidinovalerophenone (alpha-PVP), methylenedioxyprovalerone (MDPV) and methedrone by human liver microsomes and human liver cytosol

Analytical and bioanalytical chemistry - ISSN 1618-2642 - 407:19(2015), p. 5803-5816

Full text (Publishers DOI): <http://dx.doi.org/doi:10.1007/s00216-015-8763-6>

To cite this reference: <http://hdl.handle.net/10067/1271560151162165141>

***In vitro* Phase I and Phase II metabolism of α -pyrrolidinovalerophenone (α -PVP),
methylenedioxypropylvalerone (MDPV) and methedrone by human liver
microsomes and human liver cytosol**

Noelia Negreira^a, Claudio Erratico^a, Tina Kosjek^b, Alexander L.N. van Nuijs^a, Ester
Heath^b, Hugo Neels^a, Adrian Covaci^{a*}

^aToxicological Center, University of Antwerp, Department of Pharmaceutical Sciences,
Universiteitsplein 1, 2610 Antwerp, Belgium

^bJozêf Stefan Institute, Department of Environmental Sciences, Jamova 39, 1000
Ljubljana, Slovenia

*Corresponding authors' details:

Dr. Adrian Covaci, Toxicological Center, Universiteit Antwerpen, Universiteitsplein 1,
2610, Wilrijk-Antwerpen, Belgium.

Tel.: +32 3 265 24 98; E-mail: adrian.covaci@uantwerpen.be

1 **Abstract**

2 The aim of the present study was to identify the *in vitro* Phase I and Phase II
3 metabolites of three new psychoactive substances, e.g., α -pyrrolidinovalerophenone
4 (α -PVP), methylenedioxypropylvalerone (MDPV) and methedrone, using human liver
5 microsomes and human liver cytosol. Accurate-mass spectra of metabolites were
6 obtained using liquid chromatography-quadrupole time-of-flight mass spectrometry. Six
7 Phase I metabolites of α -PVP were identified, which were formed involving reduction,
8 hydroxylation and pyrrolidine ring opening reactions. The lactam compound was the
9 major metabolite observed for α -PVP. Two glucuronidated metabolites of α -PVP, not
10 reported in previous *in vitro* studies, were further identified. MDPV was transformed
11 into ten Phase I metabolites involving reduction, hydroxylation and loss of the
12 pyrrolidine ring. Also, six glucuronidated and two sulphated metabolites were detected.
13 The major metabolite of MDPV was the catechol metabolite. Methedrone was
14 transformed into five Phase I metabolites, involving *N*- and *O*-demethylation,
15 hydroxylation and reduction of the ketone group. Three metabolites of methedrone are
16 reported for the first time. In addition, the contribution of individual human CYP
17 enzymes in the formation of the detected metabolites was investigated.

18

19 **Keywords:** Cathinones, quadrupole time-of-flight mass spectrometry, *in vitro*
20 metabolism, MDPV, Methedrone, α -PVP, new psychoactive substances

21

22 **Introduction**

23 An increasing number of new psychoactive substances (NPS) have been recently introduced
24 onto the drug market [1]. These NPS are mostly synthetic and mimic the effects of
25 conventional illicit drugs (e.g. cannabis, amphetamines, cocaine, etc.), sometimes by simply
26 adding or changing a functional group of already known psychoactive substances [1,2].
27 Among them, the presence of synthetic cathinones on the European drug market was noted
28 for the first time in 2009 [3]. Synthetic cathinones are a group of derivatives of cathinone, a
29 phenylalkylamine alkaloid naturally present in *Catha edulis* [4-6]. Cathinone causes
30 amphetamine-like sympathomimetic effects, including tachycardia and hypertension as well
31 as psychoactive effects such as euphoria and increased alertness [1].

32 One of the most known synthetic cathinones is methylenedioxy-pyrovalerone (MDPV), a
33 potent monoamine transporter blocker with stimulating effects [7,8]. Several MDPV
34 analogues have appeared on the market, including the popular and widespread α -
35 pyrrolidinovalerophenone (α -PVP) [9]. Besides MDPV, mephedrone (4-methyl-
36 methcathinone) was also one of the first introduced and most used NPS [10], but recently, its
37 demand decreased because of legislative actions and an analogue, known as methedrone
38 (4-methoxy methylcathinone), has entered the market [11-12]. In spite of their recent
39 introduction, deaths associated with the use of these NPS were already reported [13-18].

40 NPS may undergo extensive metabolism in the body, leading to low or even negligible levels
41 of the parent compound in urine [19]. For this, the detection and quantification of metabolites
42 constitutes, in many cases, the only possible way to get useful information on the use of
43 these substances. To this end, the use of *in vitro* metabolism experimental setups, using
44 human liver microsomes (HLM) and high-performance liquid chromatography (HPLC)
45 coupled to accurate-mass mass spectrometry (AMMS) has proven to be a useful approach
46 for the characterization of the metabolism of MDPV [20,21] and α -PVP [22]. However, AMMS
47 was not used in the case of methedrone.

48 Although some information on the *in vitro* metabolism of MDPV, α -PVP and methedrone is
49 available, several and important research gaps are still present. First, out of the twelve
50 Phase I metabolites MDPV detected in a urine sample from an MDPV user [21], only two
51 were identified *in vitro* human metabolism [20]. Second, out of the seven Phase I
52 metabolites detected in urine samples from α -PVP users [23], five were confirmed in *in vitro*
53 experiments [22]. Third, CYP-mediated *in vitro* metabolism of methedrone was investigated
54 [24] and two metabolites were identified, one of which was also found in urine samples from
55 two fatal intoxications [13]. However, the confirmation of these metabolites was not done by
56 AMMS. In addition, no Phase II metabolism was investigated *in vitro* or *in vivo* for α -PVP and
57 methedrone. Cytochrome-P450 (CYP) enzymes involved in the formation of Phase I
58 metabolites was investigated only for major MDPV metabolites identified [21]. Full
59 characterization of the *in vitro* metabolism pathway of drugs is of key importance because
60 their Phase I and Phase II metabolites are the most likely urinary biomarkers of human drug
61 consumption. The identification of the (CYP) enzymes involved in drug metabolism is also of
62 great importance to describe (and predict) drug-to-drug interaction and sublethal effects.

63 To address these issues, the aim of this study was to investigate the *in vitro* Phase I and
64 Phase II metabolism of MDPV, α -PVP and methedrone by HLM and human liver cytosol
65 (HLCYT). Metabolites were identified through liquid chromatography coupled to accurate
66 mass spectrometry measurements using QTOF. In addition, the involvement of individual
67 human CYP enzymes in the formation of Phase I metabolites was studied using a panel of
68 human recombinant CYPs (rCYPs).

69

70 **Material and methods**

71 **Chemicals and reagents**

72 Chemical standards of α -PVP and methedrone were obtained from Cerilliant (Texas, U.S.) at
73 a concentration of 1 mg/mL in methanol, whereas MDPV was purchased from TRC (Toronto,
74 Canada) in neat powder. The internal standard, theophylline, was obtained as powder

75 (anhydrous, >99% pure) from Sigma-Aldrich (Diegem, Belgium). Pooled HLM (mix gender,
76 n=200) were purchased from Tebu-bio (Boechout, Belgium). Pooled HLCYT (mix gender,
77 n=200), chemical standards for 2,6-uridinediphosphate glucuronic acid (UDPGA),
78 alamethicin (neat, purity>99%), adenosine 3'-phosphate 5'-phosphosulphate (PAPS; neat,
79 purity>60%) lithium salt hydrate, 4-nitrophenol (4-NP), 4-nitrophenol-glucuronide (4-NP-Gluc;
80 neat, purity>99%), 4-nitrophenol-sulphate (4-NP-Sulf; neat, purity>99%) and NADPH (neat,
81 purity>99%) were purchased from Sigma-Aldrich (Diegem, Belgium). Baculovirus-insect cell
82 microsomes containing expressed human CYP enzyme (CYP1A2, 2B6, 2C9, 2C19, 2D6,
83 2E1 or 3A4) coexpressed with human CYP oxidoreductase and human cytochrome b5 were
84 purchased from BD Biosciences (Erembodegem, Belgium) and Tebu-Bio. Ultrapure water
85 was obtained using a Purelab flex water system by Elga (Tienen, Belgium). Acetonitrile and
86 formic acid were purchased from Merck (Darmstadt, Germany). All organic solvents were
87 HPLC grade or higher.

88

89 ***In vitro* metabolism assays**

90 The formation of Phase I metabolites by CYP enzymes was studied. The reaction mixture
91 (final volume: 1 mL), consisting of 100 mM TRIS-HCl buffer (pH adjusted to 7.4 at 37 °C),
92 HLM (final concentration: 0.5 mg/mL) and the individual drug (final concentration: 10 µM)
93 was prepared on ice and then pre-incubated for 5 min in a shaking water bath at 37 °C. The
94 reaction was initiated by addition of 10 µL of NADPH solution (final concentration: 1 mM) in
95 the mixture. To stop the reaction after 3 h, 250 µL of an ice-cold acetonitrile solution
96 containing 1% formic acid and 5.0 µg/mL of theophylline (used as internal standard) was
97 added to each sample, which was then vortex-mixed for 30 s and centrifuged at 8,000 rpm
98 for 5 min. The supernatant was then transferred to a glass tube, concentrated to dryness
99 under a gentle stream of nitrogen gas at 60 °C and reconstituted with 200 µL ultrapure water
100 before transferring it to an HPLC vial for analysis.

101 The formation of Phase II metabolites was investigated in two steps. First, Phase I
102 metabolites were produced by incubating substances with HLMs and NADPH as described

103 above. This reaction was quenched by putting the samples on ice for 5 min. Samples were
104 then centrifuged at 8,000 rpm for 5 min and 940 μ L of the supernatant containing the fraction
105 of non-metabolized drug and its formed Phase I metabolites was transferred to a tube
106 containing fresh pooled HLM or pooled HLCYT (final concentration: 0.5 mg/mL) to
107 investigate uridinediphosphate glucuronic acid transferase (UGT) or sulfotransferase (SULT)
108 mediated metabolism, respectively. The reaction mixture was prepared as described above
109 for CYP enzyme samples, but adding (only in the samples focusing on UGT enzymes) a 10
110 μ L aliquot of alamethicin (final concentration: 10 μ g/mL) dissolved in dimethyl sulphoxide (1%
111 DMSO, final concentration) before pre-incubating the samples in the water bath. Also, the
112 reaction was started by addition of UDPGA or PAPS co-factors (1 mM, final concentration) to
113 activate UGTs and SULTs, respectively. Samples were incubated for three hours and further
114 prepared as described above.

115 Further experiments were carried out by incubating the substances with HLM over a range of
116 incubation times (10, 20, 40, 60, and 90 min), enzyme concentrations (0.2, 0.4, 0.6, and 0.8
117 mg/mL) and substrate concentrations (1, 3, 5, and 10 μ M) to monitor the consistent formation
118 of Phase I metabolites over a range of different incubation conditions.

119 Positive and negative control samples for each enzyme family were prepared under the
120 same conditions as earlier described in order to assure adequate experimental procedures.
121 In the positive control samples for UGT and SULT activity, 4-nitrophenol was selected as
122 substrate and formation of 4-nitrophenol-glucuronide [25] and 4-nitrophenol-sulphate [26],
123 respectively, was monitored. Positive control samples were not prepared for CYP enzymes
124 because the activity of the major ten CYPs present in HLM was previously characterized by
125 the manufacturer (data not shown). Negative control samples were prepared for each family
126 of enzymes by replacing enzymes, substrate or the cofactor with an equivalent aliquot of
127 buffer or acetonitrile in order to avoid false-positive results .

128 The role of individual human CYP enzymes was investigated using a panel of human rCYPs,
129 including human rCYP1A2, 2B6, 2C9, 2C19, 2D6, 2E1 and 3A4. Reaction mixtures were
130 prepared as described above, but using one human rCYP (20 pmol/mL, final concentration)

131 instead of HLMs. The reaction was allowed to proceed for one hour. Negative control
132 samples were prepared replacing the human rCYP with an equivalent aliquot of buffer.

133

134 **Liquid chromatography accurate-mass spectrometry**

135 Identification of potential metabolites was performed using LC coupled to a QTOF-MS with
136 electrospray ionisation (ESI). The apparatus consisted of a 1290 Infinity LC (Agilent
137 Technologies, Wilmington, DE, USA) connected to a 6530 Accurate-Mass QTOF-MS (Agilent
138 Technologies, Wilmington, DE, USA) with a heated-ESI source (JetStream ESI).

139 Chromatographic separation was performed on a C₈ Zorbax Eclipse Plus column (150 x 2.1
140 mm, 3.5 μm) from Agilent Technologies, maintained at 30 °C, and using a mobile phase
141 composed of 0.1% of formic acid in ultrapure water (A) and acetonitrile (B) with the following
142 gradient: 0–5 min: 3% B; 5-30 min: 3-50% B; 30-31 min: 50-100% B; 31-33 min: 100% B; 33-
143 34 min: 100-3% B; 34-40 min: 3% B. The flow rate and the injection volume were set at 0.18
144 mL/min and 5 μL, respectively.

145 The QTOF-MS instrument was operated in the 2 GHz (extended dynamic range) mode,
146 which provides a full width at half maximum (FWHM) resolution of approximately 4700 at m/z
147 118 and 10000 at m/z 922. Both polarity ESI modes were used under the following specific
148 conditions: gas temperature 300 °C; gas flow 8 L/min; nebulizer pressure 40 psi; sheath gas
149 temperature 325 °C; sheath gas flow 11 L/min. Capillary and fragmentor voltages were set to
150 3500 and 100 V, respectively. A reference calibration solution (provided by Agilent
151 Technologies) was continuously sprayed into the ESI source of the QTOF-MS system. The
152 ions selected for recalibrating the mass axis, ensuring the mass accuracy throughout the run
153 were m/z 121.0508 and 922.0097 for positive mode and m/z 112.9856 and 966.0007 for
154 negative mode. The QTOF-MS device was acquiring from m/z 50 to 1000 in MS mode and
155 from m/z 40 to 500 in data-dependent acquisition mode (auto-MS/MS) using three different
156 collision energies (10, 20, and 40 eV) for the fragmentation of the selected parent ions. The
157 maximum number of precursors per MS cycle was set to three with minimal abundance of
158 2000 counts. In addition, precursor ions were excluded after every three spectra and

159 released after 0.6 min. An exclusion list with ions present in the substrate negative control
160 was also used. For some metabolites, additional injections in targeted MS/MS were
161 necessary in order to obtain proper MS/MS fragmentation data.

162

163 **Post-acquisition data processing**

164 Metabolite identification was based on mass accuracy and isotopic abundance obtained in
165 MS mode, on the MS/MS fragmentation patterns and the accurate masses of the product
166 ions, and on the predicted $\log K_{ow}$ by ChemBio3D Ultra. The MassHunter Workstation
167 software (Agilent Technologies) and XCMS online (open-source software from Scripps
168 Centre for Metabolomics) were used to process the obtained data and to provide an
169 automated detection of metabolites, respectively. The XCMS software aligns the total ion
170 current chromatograms (TICCs) corresponding to the negative controls and to the samples,
171 and determines if there is a statistically significant difference between control and sample. A
172 complete workflow can be found elsewhere [27]. A list of putative metabolites is proposed
173 and the change in response between the control and real samples can be visualized on
174 extracted ion chromatograms. Following this automated analysis, the raw data were
175 examined by manual processing in MassHunter, using a mass window of 10 ppm around the
176 precursor ion. Nexus v1.5 (Lhasa Limited) software was also considered in order to have a
177 first prediction of plausible metabolites.

178

179 **Results and discussion**

180 **Detection and identification of metabolites**

181 TICCs of the samples were compared with negative controls. Visual inspection of these
182 chromatograms showed no clear differences between them. Thus, in order to facilitate this
183 search and speed it up the data analysis, a workflow based on the the XCMS software was
184 applied. The identified metabolites of α -PVP, MDPV and methedrone are listed in Tables 1-3,
185 respectively. Sulphated metabolites were analysed in negative mode, while all other
186 metabolites were analysed in positive mode. The chemical structure of the detected

187 metabolites was postulated by interpretation of the mass shifts in the MS/MS spectra in
188 relation to the MS/MS spectrum of the parent compound and in accordance to previously
189 published data [21-23,28-30]. Fig S1-S3 show the MS/MS spectra of the three substances
190 and their detected metabolites. Extracted ion chromatograms (EICs) of the identified
191 metabolites are showed in Fig S4-S6.

192

193 **α -PVP**

194 The fragmentation pattern of α -PVP was in agreement with previously published data [31]
195 with major fragments observed at m/z 126.1271 ($\Delta m = -4.76$ ppm), 105.0333 ($\Delta m = -1.90$
196 ppm), 91.0540 ($\Delta m = -2.20$ ppm) and 77.0385 ($\Delta m = -1.30$ ppm) (Fig S1).

197 The *in vitro* CYP-catalysed metabolism for α -PVP yielded six potential metabolites (Table 1
198 and Fig S1). Metabolite M1 was formed through a transformation of the pyrrolidine ring into a
199 primary amine, resulting in m/z 178.1226 ($\Delta m = 3.31$ ppm). This metabolite was also
200 detected in the *in vitro* study performed by Tyrkkö et al. [22] and in rat urine by Sauer et al.
201 [29], but not in human urine [22,23]. Uralets et al. [31] did not find M1 in human urine, but
202 they found a metabolite formed after reduction of the ketone group leading to an alcohol. The
203 fragmentation pattern of M1 and α -PVP have similarities as evidenced from the presence of
204 m/z 105.0350 ($\Delta m = 14.28$ ppm) and 91.0560 ($\Delta m = 19.77$ ppm). However, the most
205 abundant fragments at m/z 160.1134 ($\Delta m = 8.12$ ppm) and 130.0831 ($\Delta m = 5.38$ ppm) are
206 specific for M1 (Table 1 and Fig. S1)

207

208 M2 was formed through a combination of reactions: a reduction/hydrogenation of α -PVP, a
209 hydroxylation of the pyrrolidine ring, followed by an oxidation and ring opening with an
210 additional hydroxylation. The fragments at m/z 248.1649 ($\Delta m = 1.61$ ppm) and 230.1551 (Δm
211 = 5.21 ppm) showed two successive and very favourable losses of water which means that
212 the structure contained two secondary hydroxyl groups. An additional loss of a CO moiety at
213 m/z 202.1628 ($\Delta m = 18.80$ ppm) indicated the existence of an aldehyde group. The fragment
214 at m/z 188.1066 ($\Delta m = -2.13$ ppm) is due to the loss of the propyl side chain from m/z

215 230.1551, indicating that the aldehyde group was located in the longer chain. At the same
216 time, only a double bond was present suggesting that the other hydroxylation took place in
217 the propyl side chain. To the best of our knowledge, M2 is reported for the first time in the
218 present study.

219
220 M3 (m/z 248.1650, $\Delta m = 2.10$ ppm) corresponded to the reduction of α -PVP combined with a
221 hydroxylation in the pyrrolidine ring and a subsequent oxidation. A minor peak of M3
222 detected just before M3 and with an identical MS/MS spectrum, indicated isomerism as
223 previously reported in HLM experiments [22] and in human [23] and rat urine [29].

224
225 M4 (m/z 250.1807, $\Delta m = 2.28$ ppm) was formed from α -PVP through a reduction and a
226 hydroxylation. This metabolite was also reported in the study by Tyrkkö et al. [22], but
227 information about its fragmentation pattern was lacking. The fragments at m/z 232.1721 (Δm
228 = 10.77 ppm) and 214.1608 ($\Delta m = 8.40$ ppm) indicated the loss of one and two water
229 molecules, respectively. Subsequently, the loss of the propyl side chain (m/z 172.1132, $\Delta m =$
230 6.39 ppm), the pyrrolidine ring (m/z 160.1142, $\Delta m = 13.12$ ppm) or both (m/z 130.0672, $\Delta m =$
231 16.15 ppm and m/z 118.0665, $\Delta m = 11.86$ ppm) were observed. The ions at m/z 105.0355
232 ($\Delta m = 19.04$ ppm), 91.0561 ($\Delta m = 20.87$ ppm) and 77.0409 ($\Delta m = 29.86$ ppm) were similar
233 to the α -PVP MS/MS spectrum. In some cases, the mass errors were higher than 20 ppm,
234 probably due to the low abundance observed for this metabolite. M4 was not identified in
235 human [22] and rat urine [29] samples, suggesting a minor role of this metabolite *in vivo*.

236
237 The formation of M5 (m/z 264.1599, $\Delta m = 1.93$ ppm) from α -PVP can be explained from a
238 combination of reactions: a hydroxylation of the pyrrolidine ring, an oxidation, a ring opening
239 and an additional hydroxylation. Tyrkkö et al. [22] observed the same exact mass in their *in*
240 *vitro* experiments, but the structure was assigned to the formation of a carboxylic acid due to
241 a loss of water, acetic acid and amino-butyric acid. In our case, only the loss of water was
242 faintly observed at m/z 246.1471 ($\Delta m = -7.31$ ppm) but the other losses, including a possible

243 loss of CO₂, were not seen. The fragment at *m/z* 186.0910 ($\Delta m = -1.61$ ppm) indicated that
244 the hydroxyl and carbonyl groups were in the aminobutyl side chain due to the presence of
245 two double bonds. However, the exact position of the hydroxyl group could not be elucidated.

246
247 M6 (*m/z* 234.1858, $\Delta m = 2.52$ ppm) was formed through a reduction of the ketone moiety of
248 α -PVP. A loss of water and a subsequent loss of the propyl side chain as a cation radical led
249 to ions at *m/z* 216.1726 ($\Delta m = -9.71$ ppm) and 173.1176 ($\Delta m = -13.29$ ppm), respectively, as
250 previously reported by Tyrkkö et al. [22]. The presence of the ion at *m/z* 72.0801 ($\Delta m = -9.71$
251 ppm) supports the hypothesis that the pyrrolidine ring remained unaltered here. This
252 metabolite was the most abundant metabolite found in *in vitro* [22] and *in vivo* [22-23]
253 studies.

254 An additional metabolite (*m/z* 246.1489), formed by a hydroxylation followed by a
255 dehydrogenation, was reported in *in vitro* experiments [22] and was also observed in human
256 urine [23]. This metabolite was however not observed in the present study, but it could be
257 formed as an intermediate between the parent compound and M5. In addition, the oxidation
258 of the two hydroxyl groups led to *m/z* 250.18073 observed in our study (M4). Drug and
259 protein concentrations used in the *in vitro* experiments by Tyrkkö et al. [22] (100 μ M and 2
260 mg/mL, respectively) were higher than those used in the present study (10 μ M and 0.5
261 mg/mL) and our incubation time was shorter. Therefore, differences in experimental setups
262 used in different *in vitro* metabolism studies could explain the observed differences.

263
264 In addition, two putative glucuronide conjugations of M3 were detected in the Phase II
265 experiments. Both metabolites eluted earlier than M3 with *m/z* 424.1996 ($\Delta m = 7.07$ ppm)
266 and 424.2008 ($\Delta m = 9.90$ ppm). The presence of both metabolites could be a result of
267 isomerism of M3, but they also can originate from two different bonds with the glucuronic
268 acid by a mechanism known as acyl migration [32]. However, no evidence could be found in
269 the MS/MS spectra to support this hypothesis. The fragmentation pattern of the
270 glucuronidated M3 was characterized through the neutral loss of *m/z* 176 (a glucuronyl

271 group) resulting in M3 at m/z 248.1593 ($\Delta m = -20.95$ ppm) and 248.1602 ($\Delta m = -17.33$ ppm)
272 for isomer one and two, respectively. In addition, the characteristic fragments of M3 (m/z
273 230, 105 and 91) were also observed for these glucuronidated conjugates. The mass errors
274 were higher than for Phase I metabolites, because the intensity of these conjugated
275 compounds was very low. To the best of our knowledge, the glucuronidated conjugate of M3
276 was not detected before in *in vitro* or *in vivo* studies. On the other hand, the glucuronidated
277 conjugate of M6 was found in human urine [23], but not in the present study.

278 Sulphated conjugates of α -PVP were not detected in the Phase II experiments. However, the
279 metabolite of 4-NP produced by SULTs (4-NP-SULF) was detected in the positive control
280 sample, demonstrating a good experimental setup and suggesting that sulphation did not
281 occur.

282

283 **MDPV**

284 The fragmentation pattern for MDPV (Fig S2) was in agreement with previously published
285 data [12,20-21,28]. The following paragraphs describe the identified metabolites in detail
286 (Table 2 and Fig S2).

287 M1 (m/z 280.1544, $\Delta m = 0.36$ ppm) resulted from MDPV through a loss of the methylene
288 group and subsequent hydroxylation. A loss of water at m/z 262.1458 ($\Delta m = 7.63$ ppm),
289 followed by subsequent losses, including a loss of methanol at m/z 109.0283 ($\Delta m = -0.92$
290 ppm) and the pyrrolidine ring unaltered at m/z 72.0813 ($\Delta m = 6.94$ ppm) evidenced that the
291 hydroxylation took place in the alkyl side chain. The loss of the methylene group was
292 indicated by the lack of fragments at m/z 149 and 135, present in the MS/MS spectrum of
293 MDPV. This metabolite was observed in human urine [21,33], but not in studies investigating
294 the *in vitro* human metabolism of MDPV [21].

295

296 M2 (m/z 264.1605, $\Delta m = 2.27$ ppm) corresponded to the loss of the methylene group of
297 MDPV. M2 was the major metabolite of MDPV, which was consistent with previous *in vitro*
298 [20] and *in vivo* [21,33] studies. The most abundant ions at m/z 175.0762 ($\Delta m = 4.57$ ppm),

299 137.0246 ($\Delta m = 9.49$ ppm), 126.1291 ($\Delta m = 11.10$ ppm), 123.0454 ($\Delta m = 10.57$ ppm), and
300 109.0302 ($\Delta m = 16.51$ ppm) were already elucidated by Meyer et al. [21].

301
302 M3 (m/z 262.1434, $\Delta m = 0.38$ ppm) was formed from the parent compound by a loss of the
303 methylene group followed by a dehydrogenation in the alkyl chain. Alternatively, it could also
304 be the result from a dehydration of M1. The lack of ions at m/z 149 and 135 supported the
305 loss of the methylene moiety in the precursor ion. Several ions indicated the formation of a
306 double bond. For instance, the ion at m/z 220.0987 ($\Delta m = 8.63$ ppm) corresponded to the
307 loss of a propylene moiety (C_3H_6) instead of a propyl group (C_3H_8). The ion at m/z 178.0514
308 ($\Delta m = 8.42$ ppm) may indicate the loss of the pyrrolidine ring and an ethylene moiety. The
309 fragmentation resulting in an ion at m/z 145.0662 ($\Delta m = 9.65$ ppm) can be explained by the
310 losses of two hydroxyl groups, the pyrrolidine ring and a methane moiety. A subsequent loss
311 of water yielded the ion at m/z 127.0547 ($\Delta m = 3.94$ ppm), which can be explained by the
312 formation of a naphthalene ring. Successive fragmentations in the naphthalene ring led to
313 different ions also observed in the metabolites as explained above. To the best of our
314 knowledge, the formation of M3 is reported for the first time.

315
316 M4 (m/z 310.1636, $\Delta m = -4.19$ ppm) was formed after a reduction of the ketone moiety of
317 MDPV followed by two hydroxylations: one in the propyl chain and one in the α -position to
318 the nitrogen atom. A subsequent oxidation of the latter hydroxyl group caused a ring
319 opening. Two consecutive water losses at m/z 292.1556 ($\Delta m = 4.45$ ppm) and 274.1461 (Δm
320 = 8.39 ppm) and a subsequent loss of CO at m/z 246.1493 ($\Delta m = 1.63$ ppm) indicated the
321 presence of two hydroxyl groups and an aldehyde group. An additional ion at m/z 71.0498
322 ($\Delta m = 9.85$ ppm) demonstrated the existence of an aldehyde group in the N-butyl side chain
323 of the parent ion which indicates ring opening. The fragment at m/z 149.0243 ($\Delta m = 6.71$
324 ppm) showed the presence of the methylenedioxybenzoyl moiety similar to MDPV. To the
325 best of our knowledge, formation of M4 is reported for the first time.

326

327 M5 (m/z 222.1120, $\Delta m = -5.85$ ppm) resulted from the transformation of the pyrrolidine ring
328 of MDPV to a primary amine. The first ion at m/z 204.1002 ($\Delta m = -8.33$ ppm) corresponded
329 to a loss of water and can be explained by the formation of a conjugated indole system
330 between the primary amine and the aromatic ring, similar to that observed for M1 of α -PVP.
331 Subsequent losses of a methyleneoxy and methylenedioxy moiety led to the ions at m/z
332 174.0900 ($\Delta m = -7.47$ ppm) and 146.0941 ($\Delta m = -15.74$ ppm), respectively. An additional
333 loss of the propyl radical yielded the ion at m/z 117.0552 ($\Delta m = -17.94$ ppm). The ion at m/z
334 135.0426 ($\Delta m = -11.11$ ppm) showed the presence of the unchanged methylenedioxy
335 moiety. To the best of our knowledge, this metabolite was not previously reported *in vitro* or
336 *in vivo* metabolism studies of MDPV.

337

338 M6 (m/z 260.1272, $\Delta m = -3.46$ ppm) corresponded to the loss of the methylene group
339 followed by two dehydrogenations. MS/MS fragmentation suggested a loss of the C_2H_6
340 moiety (m/z 230.0812, $\Delta m = 0.00$ ppm) followed by a loss of CO (m/z 202.0851, $\Delta m = -5.94$
341 ppm), respectively. The ion at m/z 202 fragmented further to the ion at m/z 156.0799 ($\Delta m = -$
342 5.77 ppm) after ring opening and formation of a bond between the nitrogen atom and the
343 phenyl ring, yielding an indole system.

344

345 M7 (m/z 292.1547, $\Delta m = 1.37$ ppm) corresponded to a hydroxylation of MDPV. A loss of
346 water was observed at m/z 274.1467 ($\Delta m = 10.58$ ppm). The ion at m/z 205.0853 ($\Delta m = -$
347 2.93 ppm) suggested a hydroxylation of the pyrrolidine ring due to the lack of a double bond
348 in this fragment. The existence of the ions at m/z 149.0243 ($\Delta m = 6.71$ ppm), 135.0454 (Δm
349 = 7.40 ppm) and 121.0299 ($\Delta m = 4.13$ ppm) showed the presence of the unchanged
350 methylenedioxybenzoyl moiety. This metabolite was detected as a product of microbial
351 biotransformation in wastewater [28], but not in human *in vitro* and *in vivo* metabolism
352 experiments. Therefore, M7 is reported for the first time to be an *in vitro* metabolite of MDPV
353 in humans. Meyer et al. [21] attributed the m/z 292.1534 to the demethylenyl-methyl-oxo-

354 metabolite in human urine. The ions at m/z 151.0389 and 140.1069 appeared in their
355 spectrum [21] instead of 149 and 142.

356
357 M8 (m/z 294.1697, $\Delta m = -1.02$ ppm) is formed from MDPV through a hydrogenation followed
358 by a hydroxylation. It was indicated by two consecutive losses of water at m/z 276.1583 (Δm
359 $= -3.98$ ppm) and 258.1461 ($\Delta m = -10.85$ ppm). Subsequently, the methylene group was lost
360 yielding ion at m/z 246.1491 ($\Delta m = 0.81$ ppm). After that, two possible fragments at m/z
361 204.1012 ($\Delta m = -3.43$ ppm) could correspond to the loss of the propyl side chain from 246 or
362 the loss of the pyrrolidine ring from 258 after breaking up the bond between the nitrogen
363 atom and its carbon in α -position. The ions at m/z 149.0236 ($\Delta m = 2.01$ ppm) and 135.0439
364 ($\Delta m = -1.48$ ppm) showed the presence of the unchanged methylenedioxybenzoyl moiety.
365 Mardal and Meyer [28] attributed the same exact mass to another transformation product
366 (hydroxylation in the propyl side chain and ring opening), despite the fact that they obtained
367 the same MS/MS spectrum. This equivocal assignment was due to the fact that only the
368 structures of the fragments at m/z 204.1019 and 174.0913 were elucidated and that the two
369 losses of water were ignored [28]. Meyer et al. [21] found another metabolite in human urine
370 with the same exact mass than M8, but with a totally different fragmentation pattern
371 corresponding to the demethylenyl-methyl-hydroxy-alkyl-MDPV. Bertol et al. [33] assigned
372 the same metabolite, also in human urine, following the proposal of Meyer et al. [21], but the
373 MS/MS spectrum was not presented. Therefore, careful evaluation of the MS/MS spectrum
374 and proper interpretation of the product ions is very important to reliably identify the structure
375 of the metabolites.

376
377 M9 (m/z 308.1495, $\Delta m = -0.97$ ppm) corresponded to a di-hydroxylation of MDPV. Two
378 losses of water at m/z 290.1397 ($\Delta m = 3.45$ ppm) and 272.1275 ($\Delta m = -2.20$ ppm) indicated
379 the presence of two hydroxyl groups. A subsequent loss of a methylene group or the propyl
380 side chain led to the ions at m/z 260.1279 ($\Delta m = -0.77$ ppm) and 230.0826 ($\Delta m = 6.08$ ppm),
381 respectively. The ion at m/z 272 was fragmented following two different ways. It lost the

382 methylenedioxy moiety and a methyl group from the propyl side chain yielding ion at m/z
383 214.1227 ($\Delta m = 0.47$ ppm) or it lost the ring pyrrolidine and the hydroxyl group from the
384 ketone moiety leading to the ion at m/z 187.0758 ($\Delta m = 2.14$ ppm). The ions at m/z 149.0234
385 ($\Delta m = 0.67$ ppm) and 135.0441 ($\Delta m = 0.00$ ppm) demonstrated the unchanged
386 methylenedioxy moiety. The presence of the ion at m/z 140.1073 ($\Delta m = 2.14$ ppm), with 2 u
387 of difference compared to the ion at m/z 142 showed for M7, indicated the existence of a
388 double bond in the pyrrolidine ring or in the propyl side chain, probably due to the presence
389 of a hydroxyl group. This metabolite was not found previously in *in vitro* [20] and *in vivo*
390 [21,33] experiments. However, evidence of the formation of this compound can be found in
391 the work of Mardal and Meyer [28] where the TOF-MS spectrum was assigned to the
392 hydroxyl-alkyl-oxo-N-dealkyl transformation product despite the fact that they also observed
393 two losses of water.

394
395 M10 (m/z 278.1733, $\Delta m = -6.47$ ppm) was formed through the hydrogenation of MDPV. The
396 fragmentation pattern showed mainly a loss of water at m/z 260.1678 ($\Delta m = 12.68$ ppm) and
397 a subsequent loss of a propyl radical at m/z 217.1126 ($\Delta m = 13.36$ ppm), in accordance with
398 Paul et al. [30] who elucidated the structure of the same metabolite in human urine. A
399 comparable MS/MS spectrum was reported in an *in vitro* metabolism study [20], but in our
400 opinion the structure of the metabolite was assigned equivocally to methylcatechol-MDPV, in
401 spite of the fact that the same ions were observed in the MS/MS spectrum. Meyer et al. [21]
402 found two metabolites in human and rat urine with the same exact mass but different
403 fragmentation, so it was attributed to methyl-catechol and demethylenyl-oxo- MDPV.

404 In the Phase II experiments, glucuronidated conjugates of M2, M3 and M6 were detected, as
405 well as sulphated conjugates of M2. In each case, two isomers were detected resulting from
406 the presence of two hydroxyl groups located on the aromatic ring. The mass errors and, the
407 proposed molecular formulas and structures can be found in Table 2. The MS/MS spectra
408 (Fig S2) showed that the main fragments of the conjugates could be assigned to their non-
409 conjugated equivalent (being M2, M3 and M6). To the best of our knowledge, this is the first

410 study reporting the glucuronidated conjugates of M3 and M6. However, one of the
411 glucuronidated isomers of M2 (demethylenyl-MDPV), as well as a sulphated isomer has
412 been found in *in vitro* experiments by Strano-Rossi et al. [20]. These authors found also the
413 demethylenyl-methyl-(or methyl catechol-) MDPV-glucuronide and sulphate [20], which were
414 not observed in our study. In human urine, the demethylenyl-methyl-, demethylenyl-methyl-
415 oxo-, demethylenyl-methyl-hydroxy-, demethylenyl-oxo-, demethylenyl-hydroxy-, besides the
416 demethylenyl- and demethylenyl-methyl-glucuronide-MDPV were found by Meyer et al. [21]
417 and Bertol et al. [33], but were not observed in our study and neither by Strano-Rossi et al.
418 [20]. No sulphated metabolites of MDPV were identified in human urine [21,33].

419

420 **Methedrone**

421 The MS/MS spectrum for methedrone (Fig S3) showed the ions at m/z 176.1072 ($\Delta m = 1.14$
422 ppm) and 161.0835 ($\Delta m = 0.00$ ppm), as previously reported [3].

423 M1 (m/z 182.0816, $\Delta m = 2.20$ ppm) was formed through a *N*- and *O*-demethylation and
424 ahydroxylation . The loss of NH_3 at m/z 165.0560 ($\Delta m = 8.48$ ppm), the loss of a water
425 molecule at m/z 147.0439 ($\Delta m = -1.36$ ppm) and the loss of CH_2O_2 at m/z 136.0772 ($\Delta m =$
426 11.02 ppm) demonstrated that the hydroxylation took place in the methyl group bounded in
427 α -position to the nitrogen atom. The hydroxylation in this place was also observed for other
428 cathinones with similar structure [21]. From the ion at m/z 147, loss of CO led to the ion at
429 m/z 107.0509 ($\Delta m = 16.81$ ppm).

430

431 Two peaks corresponding to the demethylation of methedrone were observed at m/z
432 180.1018 ($\Delta m = -3.33$ ppm) and at m/z 180.1023 ($\Delta m = -0.56$ ppm) for M3 and M4,
433 respectively. Characteristic fragment ions were observed at m/z 162.0905 ($\Delta m = -4.94$ ppm)
434 and at m/z 147.0682 ($\Delta m = 2.04$ ppm) for M3 and at m/z 162.0906 ($\Delta m = -4.32$ ppm) and at
435 m/z 147.0673 ($\Delta m = -4.08$ ppm) for M4. Other fragment ions were similar to those observed
436 in the methedrone MS/MS spectrum. Taking into account the $\log K_{ow}$ estimated by
437 ChemBio3D Ultra, the first metabolite should correspond to the *N*-demethylation (M3) and

438 the second one to the *O*-demethylation (M4). These metabolites were previously found by
439 Mueller and Rentsch [24] after *in vitro* metabolism experiments of methedrone and in urine
440 from two fatal intoxications [13], but their confirmation was not done by AMS.

441
442 M5 (m/z 196.1341, $\Delta m = 2.04$ ppm) corresponded to the reduction of the ketone group of
443 methedrone. A loss of water was observed in the MS/MS spectrum at m/z 178.1230 ($\Delta m =$
444 2.25 ppm) yielding the most abundant ion. The ion at m/z 146.0958 ($\Delta m = -4.11$ ppm) was
445 observed in the methedrone spectrum as well. The rest of the fragment ions had very low
446 abundance and as such, the m/z could not be measured accurately. This metabolite was not
447 previously reported [24] although the same reaction was noted for other cathinones, such as
448 4-methylethcathinone [24] and mephedrone [34-35].

449
450 An additional metabolite (M2) at m/z 210.1121 ($\Delta m = -4.28$ ppm) corresponding to a
451 hydroxylation of methedrone was observed in full scan mode. Unfortunately, the compound
452 was not present at high abundance and no MS/MS spectrum could be acquired. Although the
453 position of the hydroxyl group could not be confirmed, it might be located in the methyl group
454 attached to the α -carbon of the nitrogen atom. If so, M2 could be a substrate for the
455 formation of M1 by *N*- and *O*-demethylation.

456
457 No glucuronidated and sulphated conjugates of methedrone and its Phase I metabolites
458 were detected. However, positive control samples confirmed the reliability of the
459 experimental design.

460

461 **Time, enzyme and substrate profiles of the metabolites detected**

462 The profiles of the identified metabolites at different incubation times, enzyme concentrations
463 and substrate concentrations are showed in the Supplementary Information (Fig S7 to S10).

464 The response of the metabolite is reported as a ratio of the peak area of the metabolite to the
465 area of the IS peak. However, it should be remarked that, although useful for discussion

466 purposes, a higher response does not always guarantee a higher concentration of the
467 metabolites as different ESI efficiencies may be expected for different chemical structures.
468 No metabolites were detected in any negative control sample and, in general, an increasing
469 trend in the response was observed with incubation time, enzyme and substrate
470 concentrations. In some cases, a decrease in the metabolite response was observed,
471 possibly because of their consequent conversion into other metabolites. In the case of
472 MDPV, the response ratios clearly suggest that M2 is the major metabolite of MDPV under
473 the experimental conditions used (Fig S8). For methedrone, the responses of M2 and M5
474 were 100 times lower than those of M3, suggesting that M2 and M5 are minor metabolites
475 (Fig S10).

476

477 **Human CYP enzymes involved in the metabolism of α -PVP, MDPV and methedrone**

478 **α -PVP**

479 All metabolites identified in the HLM experiments were also formed in human rCYP
480 incubations (Fig 1). Among the panel of rCYPs tested, rCYP2D6 was the only enzyme
481 responsible for the formation of M4, M5 and M6, and it was a major enzyme in the formation
482 of M1 and M2. rCYP2B6 and rCYP2C19 were the main enzymes responsible for the
483 formation of M1, M2 and M3. Nevertheless, the human hepatic CYP3A4, together with 2B6,
484 2C19, 2D6, were reported to catalyze the hydroxylation of the alkyl chain in α -PVP [29]. To
485 the best of our knowledge, the human hepatic CYPs responsible for the formation of all
486 metabolites, except those formed by hydroxylation, were identified here for the first time..

487

488 **MDPV**

489 With the exception of M6 and M10, all metabolites identified in the HLM experiments were
490 found in human rCYPs experiments (Fig 1). This result suggests that M6 and M10 are likely
491 formed by other enzymes present in the HLM. . Among the rCYPs tested, rCYP1A2,
492 rCYP2B6, rCYP2C9, rCYP2C19 and rCYP2D6 were the major enzymes catalysing the
493 formation of M1, M2, M3, M4, M5 and M7, whereas rCYP2D6 was the main enzyme

494 catalysing the formation of M9 and the only one involved in the formation of M8. Only the
495 rCYPs implicated in the demethylation of MDPV were previously identified [21].
496 Recombinant CYP2C19, followed by rCYP2D6 and rCYP1A2, were found to be the main
497 enzymes catalysing the formation of M2 [21]. Our data show that rCYP1A2, rCYP2C19 and
498 rCYP2D6 played an important role in the formation of M2, but also show that rCYP2B6 and
499 especially rCYP2C9 were among the most important enzymes involved in the formation of
500 M2. Differences in the experimental design, analytical methods or both could help explaining
501 differences in the human recombinant CYP enzymes found to be responsible for the
502 formation of M2.

503

504 **Methedrone**

505 With the exception of M4, all metabolites formed incubating methedrone with HLM were also
506 formed by the panel of human rCYP enzymes (Fig 1). Among the tested panel of human
507 rCYPs, rCYP2D6 was the main enzyme responsible for the *N*-demethylation of the
508 methedrone producing M3. This data is consistent with what previously reported for
509 mephedrone *in vitro* metabolism [34]. Besides rCYP2D6, rCYP1A2, rCYP2B6 and
510 rCYP2C19 were involved in the *O*-demethylation of methedrone, resulting in M4. The
511 hydroxylation of methedrone (forming M2) was catalysed almost exclusively by rCYP2C19.
512 Whereas M1 presented the same response for all rCYPs, M5 was not observed in any
513 sample and neither in the negative control. This data is consistent with M5 being a minor
514 metabolite of methedrone produced by HLM, but it could also suggest the involvement of
515 human hepatic CYP enzymes other than those tested.

516

517 **Proposed metabolic pathways for α -PVP, MDPV and methedrone**

518 A tentative metabolism pathway of the drugs of interest with CYPs is proposed in Fig 2.
519 α -PVP was found to be metabolized by a carbonyl reduction (M6), followed by a
520 hydroxylation in the pyrrolidine ring (M4), a dehydrogenation/oxidation to form a lactam
521 structure (M3), and a subsequent ring opening to form an aliphatic aldehyde combined with

522 an additional hydroxylation in the propyl side chain (M2). α -PVP could be transformed into
523 M5 after two hydroxylations in the pyrrolidine ring, one of them in α -position to the nitrogen
524 atom, followed by an oxidation with a ring opening yielding an aldehyde. Finally, M1 was
525 formed after losing the hydroxyaminobutanal chain of M5 or the pyrrolidine ring of α -PVP. We
526 observed only a glucuronidation of M3 as Phase II reactions. These findings were in
527 agreement with those reported by Tyrkkö et al. [22]. However, formation of M1 and the
528 glucuronidated conjugates of M3 are reported for the first time in the present study, together
529 with the identity of the CYP enzymes involved in the formation of the metabolites. Therefore,
530 our study represents an improvement towards the complete characterization of the pathway
531 of α -PVP metabolism and the prediction of its *in vivo* metabolism in humans. Urine is a
532 complex matrix in which the identification of metabolites by non-targeted approaches is
533 extremely difficult because of the lack of a control or blank (exactly the same matrix without
534 substance and metabolites) in order to compare with the sample from the user. For this
535 reason, the present work is very relevant in order to add these new metabolites in a
536 database and to look for them in urine samples by targeted approaches.

537 MDPV was metabolized in a large extension, with an *O*-demethylenation (M2) as most
538 favourable reaction. However, other pathways were also elucidated (Fig. 2). M2 can be
539 hydroxylated to M1 and subsequently dehydrated to M3. MDPV could also undergo a
540 hydroxylation (M7), two hydroxylations (M9), followed by *O*-demethylenation and two losses
541 of water (M6). M6 could also be formed from M3 by dehydrogenation in the pyrrolidine ring.
542 Another pathway was the reduction of the carbonyl group of MDPV (M10), followed by
543 hydroxylation in the propyl side chain (M8), hydroxylation of the pyrrolidine ring in α -position
544 to the nitrogen atom, subsequent oxidation yielding ring opening and formation of an
545 aldehyde group (M4). Finally, M5 could be formed from MDPV or M7 after a loss of the
546 pyrrolidine ring. MDPV underwent Phase II metabolism catalysed by UGTs and SULTs. In
547 particular, M2, M3 and M6 were glucuronidated yielding two isomeric conjugates, whereas
548 only M2 is sulphated.

549 Previous *in vitro* experiments carried out by Strano-Rossi et al. [20] reported that the main
550 metabolites of MDPV were the catechol and the methylcatechol, which were in turn
551 sulphated and glucuronidated. Meyer et al. [21] identified the CYP enzymes responsible for
552 only the conversion of MDPV into its catechol metabolite (M2 in the present study). All other
553 metabolites of MDPV were not described previously in *in vitro* experiments, though M1, M2
554 and M10 have been found in human urine [21,30,33]. Human rCYP enzymes involved in their
555 formation as well as discrepancies in assigning the structures of the metabolites present in
556 previous studies [21,33] were clarified. Therefore, the present study not only confirms the
557 previous limited findings about MDPV *in vitro* metabolism, but also substantially improves our
558 understanding of Phase I and Phase II *in vitro* metabolism of MDPV. Furthermore, it predicts
559 better the *in vivo* MDPV metabolism and provides a more thorough assignment of the
560 structures of the detected metabolites.

561
562 The main pathway observed for methedrone was a *N*- and *O*- demethylation resulting in M3
563 and M4. Hydroxylation of the methyl group attached to the α -carbon of the nitrogen atom
564 (M2) and reduction of the ketone group (M5) were also observed (Fig. 2). The detection of
565 small amounts of M2 can be due to its quick *N*- and *O*- demethylation leading to M1. This
566 metabolite can also be formed from M3 after *O*-demethylation and hydroxylation. These
567 results are in agreement with those described for other similar cathinones [24]. However,
568 only the formation of M3 and M4 has been reported in the sole study investigating the *in vitro*
569 metabolism of methedrone [24]. Therefore, our study confirms previous findings but it also
570 extends the characterization of the *in vitro* metabolism pathway of methedrone, including the
571 identification of the CYP enzymes involved.

572

573 **Conclusions**

574 In the present study, the *in vitro* Phase I and Phase II metabolism of α -PVP, MDPV and
575 methedrone was investigated using HLM and HLCYT. The major metabolite for MDPV was
576 the catechol, which was further glucuronidated and sulphated. α -PVP and methedrone were
577 preferentially metabolized by mono-hydroxylation after *ketone*-reduction and *N*-
578 demethylation, respectively. The difference in response between the major and the other
579 metabolites of α -PVP and methedrone was not as high as for MDPV metabolites.
580 Nevertheless, all *in vitro* metabolites should be confirmed with *in vivo* data, because the
581 prevalence of one or other metabolites may vary with the time after the intake of the drug.
582 Therefore, these results are very useful in order to generate databases as complete as
583 possible for the screening of consumption of NPS through urine analysis.

584

585 **Acknowledgements**

586 The authors thank Walid Maho and Steven Andries for technical assistance. This study has
587 been financially supported by the EU through the FP7 (2007-2013) project under grant
588 agreement #316665 (A-TEAM). Noelia Negreira and Alexander L.N. van Nuijs acknowledge
589 University of Antwerp and FWO Flanders for their respective postdoctoral fellowships.

References

1. Prosser J, Nelson L (2012) The Toxicology of Bath Salts: A Review of Synthetic Cathinones. *J Med Toxicol* 8:33-42
2. Brandt SD, King LA, Evans-Brown M (2014) The new drug phenomenon. *Drug Test Anal* 6:587-597
3. Zuba D (2012) Identification of cathinones and other active components of 'legal highs' by mass spectrometric methods. *TrAC – Trend Anal Chem* 32:15-30
4. Coppola M, Mondola R (2012) 3,4-Methylenedioxypropylvalerone (MDPV): Chemistry, pharmacology and toxicology of a new designer drug of abuse marketed online. *Toxicol Lett* 208:12-15
5. Favretto D, Pascali JP, Tagliaro F (2013) New challenges and innovation in forensic toxicology: Focus on the “New Psychoactive Substances”. *J Chromatogr A* 1287:84-95
6. Zaitsev K, Katagi M, Tsuchihashi H, Ishii A (2014) Recently abused synthetic cathinones, α -pyrrolidinophenone derivatives: a review of their pharmacology, acute toxicity, and metabolism. *Forensic Toxicol* 32:1-8
7. Baumann MH, Partilla JS, Lehner KR, Thorndike EB, Hoffman AF, Holy M, Rothman RB, Goldberg SR, Lupica CR, Sitte HH, Brandt SD, Tella SR, Cozzi NV, Schindler CW (2013) Powerful Cocaine-Like Actions of 3,4-Methylenedioxypropylvalerone (MDPV), a Principal Constituent of Psychoactive ‘Bath Salts’ Products. *Neuropsychopharmacol* 38:552-562
8. Anizan S, Ellefsen K, Concheiro M, Suzuki M, Rice KC, Baumann MH, Huestis MA (2014) 3,4-Methylenedioxypropylvalerone (MDPV) and metabolites quantification in human and rat plasma by liquid chromatography–high resolution mass spectrometry. *Anal Chim Acta* 827:54-63
9. Marusich JA, Antonazzo KR, Wiley JL, Blough BE, Partilla JS, Baumann MH (2014) Pharmacology of novel synthetic stimulants structurally related to the “bath salts” constituent 3, 4-methylenedioxypropylvalerone (MDPV). *Neuropharmacol* 87:206-213
10. Elliott S, Evans J (2014) A 3-year review of new psychoactive substances in casework. *Forensic Sci Int* 243:55-60
11. Zancajo M R, Brito J, Carrasco M P, Bronze M R, Moreira R, Lopes A (2014) Analytical profiles of “legal highs” containing cathinones available in the area of Lisbon, Portugal. *Forensic Sci Int* 244:102–110
12. Ibáñez M, Sancho JV, Bijlsma L, Van Nuijs ALN, Covaci A, Hernández F (2014) Comprehensive analytical strategies based on high-resolution time-of-flight mass spectrometry to identify new psychoactive substances. *TrAC - Trend Anal Chem* 57:107-117
13. Wikström M, Thelander G, Nyström I, Kronstrand R (2010) Two fatal intoxications with the new designer drug methedrone (4-methoxymethylcathinone). *J Anal Tox* 34:594-598
14. Hasegawa K, Suzuki O, Wurita A, Minakata K, Yamagishi I, Nozawa H, Gonmori K, Watanabe K (2014) Postmortem distribution of α -pyrrolidinopropylphenone and its metabolite in body fluids and solid tissues in a fatal poisoning case measured by LC-MS/MS with the standard addition method. *Forensic Toxicol* 32:225-234
15. Nagai H, Saka K, Nakajima M, Maeda H, Kuroda R, Igarashi A, Tsujimura-Ito T, Nara A, Komori M, Yoshida K-i (2014) Sudden death after sustained restraint following self-administration of the designer drug α -pyrrolidinopropylphenone. *Int J Cardiol* 172:263-265
16. Namera A, Urabe S, Saito T, Torikoshi-Hatano A, Shiraishi H, Arima Y, Nagao M (2013) A fatal case of 3,4-methylenedioxypropylvalerone poisoning: coexistence of α -pyrrolidinobutylphenone and α -pyrrolidinopropylphenone in blood and/or hair. *Forensic Toxicol* 31:338-343
17. Wyman JF, Lavins ES, Engelhart D, Armstrong EJ, Snell KD, Boggs PD, Taylor SM, Norris RN, Miller FP (2013) Postmortem Tissue Distribution of MDPV Following Lethal Intoxication by “Bath Salts”. *J Anal Toxicol* 37:182-185
18. Murray B, Murphy C, Beuhler M (2012) Death Following Recreational Use of Designer Drug “Bath Salts” Containing 3,4-Methylenedioxypropylvalerone (MDPV). *J Med Toxicol* 8:69-75
19. de Jager AD, Warner JV, Henman M, Ferguson W, Hall A (2012) LC–MS/MS method for the quantitation of metabolites of eight commonly-used synthetic cannabinoids in human urine – An Australian perspective. *J Chromatogr B* 897:22-31

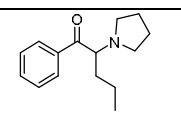
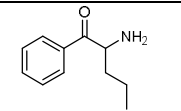
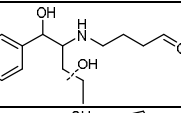
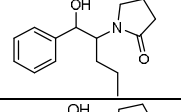
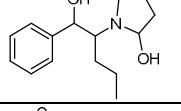
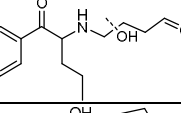
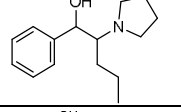
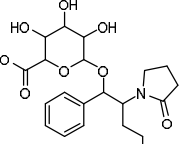
20. Strano-Rossi S, Cadwallader AB, de la Torre X, Botrè F (2010) Toxicological determination and *in vitro* metabolism of the designer drug methylenedioxypropylone (MDPV) by gas chromatography/mass spectrometry and liquid chromatography/quadrupole time-of-flight mass spectrometry. *Rapid Commun Mass Sp* 24:2706-2714
21. Meyer MR, Du P, Schuster F, Maurer HH (2010) Studies on the metabolism of the α -pyrrolidinophenone designer drug methylenedioxy-propylone (MDPV) in rat and human urine and human liver microsomes using GC-MS and LC-high-resolution MS and its detectability in urine by GC-MS. *J Mass Spectrom* 45:1426-1442
22. Tyrkkö E, Pelander A, Ketola R, Ojanperä I (2013) *In silico* and *in vitro* metabolism studies support identification of designer drugs in human urine by liquid chromatography/quadrupole-time-of-flight mass spectrometry. *Anal Bioanal Chem* 405:6697-6709
23. Shima N, Katagi M, Kamata H, Matsuta S, Sasaki K, Kamata T, Nishioka H, Miki A, Tatsuno M, Zaito K, Ishii A, Sato T, Tsuchihashi H, Suzuki K (2014) Metabolism of the newly encountered designer drug α -pyrrolidinopropylone in humans: Identification and quantitation of urinary metabolites. *Forensic Toxicol* 32:59-67
24. Mueller DM, Rentsch KM (2012) Generation of metabolites by an automated online metabolism method using human liver microsomes with subsequent identification by LC-MS (n), and metabolism of 11 cathinones. *Anal Bioanal Chem* 402:2141-2151
25. Tukey RH, Strassburg CP (2000) Human UDP-Glucuronosyltransferases: Metabolism, Expression, and Disease. *Ann Rev Pharmacol* 40:581-616
26. Gamage N, Barnett A, Hempel N, Duggleby RG, Windmill KF, Martin JL, McManus ME (2006) Human Sulfotransferases and Their Role in Chemical Metabolism. *Toxicol Sci* 90:5-22
27. Tautenhahn R, Patti GJ, Rinehart D, Siuzdak G (2012) XCMS Online: A Web-Based Platform to Process Untargeted Metabolomic Data. *Anal Chem* 84:5035-5039
28. Mardal M, Meyer MR (2014) Studies on the microbial biotransformation of the novel psychoactive substance methylenedioxypropylone (MDPV) in wastewater by means of liquid chromatography-high resolution mass spectrometry/mass spectrometry. *Sci Total Environ* 493:588-595
29. Sauer C, Peters FT, Haas C, Meyer MR, Fritschi G, Maurer HH (2009) New designer drug α -pyrrolidinopropylone (PVP): studies on its metabolism and toxicological detection in rat urine using gas chromatographic/mass spectrometric techniques. *J Mass Spectrom* 44:952-964
30. Paul M, Ippisch J, Herrmann C, Guber S, Schultis W (2014) Analysis of new designer drugs and common drugs of abuse in urine by a combined targeted and untargeted LC-HR-QTOFMS approach. *Anal Bioanal Chem* 406:4425-4441
31. Uralets V, Rana S, Morgan S, Ross W (2014) Testing for Designer Stimulants: Metabolic Profiles of 16 Synthetic Cathinones Excreted Free in Human Urine. *J Anal Toxicol* 38:233-241
32. Regan SL, Maggs JL, Hammond TG, Lambert C, Williams DP, Park BK (2010) Acyl glucuronides: the good, the bad and the ugly. *Biopharm Drug Dispos* 31:367-395
33. Bertol E, Mari F, Boscolo Berto R, Mannaioni G, Vaiano F, Favretto D (2014) A mixed MDPV and benzodiazepine intoxication in a chronic drug abuser: Determination of MDPV metabolites by LC-HRMS and discussion of the case. *Forensic Sci Int* 243:149-155
34. Pedersen A, Reitzel L, Johansen S, Linnet K (2013) *In vitro* metabolism studies on mephedrone and analysis of forensic cases. *Drug Test Anal* 5:430-438
35. Meyer MR, Wilhelm J, Peters FT, Maurer HH (2010) Beta-keto amphetamines: studies on the metabolism of the designer drug mephedrone and toxicological detection of mephedrone, butylone, and methylone in urine using gas chromatography-mass spectrometry. *Anal Bioanal Chem* 397:1225-1233

Figure captions

Fig. 1. Ratio response of α -PVP, MDPV and methedrone metabolites after 1 h-incubations of each drug at 10 μ M with a panel of human recombinant CYP enzymes (20 pmol/mL).

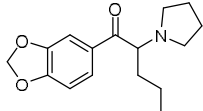
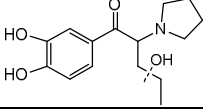
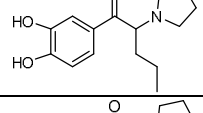
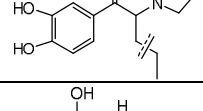
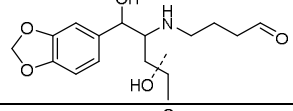
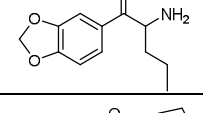
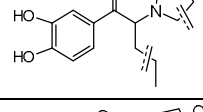
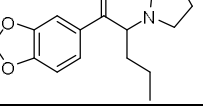
Fig. 2. Proposed metabolism pathway of α -PVP, MDPV and methedrone.

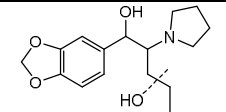
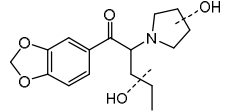
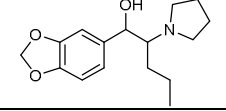
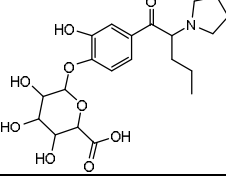
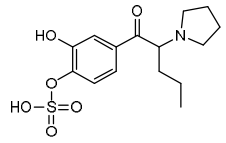
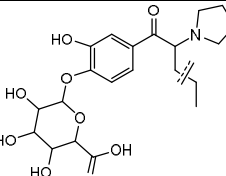
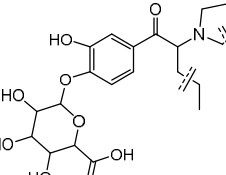
Table 1: Postulated structures for α -PVP and its Phase I and Phase II metabolites.

| Compound | Retention time (min) | Theoretical m/z [M+H] ⁺ | Measured m/z [M+H] ⁺ | Error (ppm) | Diagnostic product ions | Chemical formula | Structure | Log Kow ¹ |
|--------------------------------|----------------------|--------------------------------------|-----------------------------------|--------------|--|---|---|----------------------|
| α-PVP | 18.79 | 232.1696 | 232.1703 | 3.06 | 126.1271, 105.0333, 91.0540, 77.0385 | C ₁₅ H ₂₁ NO |  | 3.31 |
| M1 | 15.78 | 178.1226 | 178.1232 | 3.31 | 160.1134, 130.0831 | C ₁₁ H ₁₅ NO |  | 2.19 |
| M2 | 16.12 | 266.1751 | 266.1756 | 2.10 | 248.1649, 230.1551, 202.1628, 188.1066 | C ₁₅ H ₂₃ NO ₃ |  | 1.68 |
| M3 | 16.63 | 248.1645 | 248.1650 | 2.10 | 230.1532, 202.1569, 118.0657, 142.1197 | C ₁₅ H ₂₁ NO ₂ |  | 2.21 |
| M4 | 17.09 | 250.1802 | 250.1807 | 2.28 | 232.1721, 214.1608, 172.1132, 160.1142, 130.0672 | C ₁₅ H ₂₃ NO ₂ |  | 2.49 |
| M5 | 17.54 | 264.1594 | 264.1599 | 1.93 | 246.1471, 186.0910 | C ₁₅ H ₂₁ NO ₃ |  | 2.38 |
| M6 | 18.75 | 234.1852 | 234.1858 | 2.52 | 216.1726, 173.1176, 72.0801 | C ₁₅ H ₂₃ NO |  | 3.02 |
| M3-GLU | 14.66, 15.20 | 424.1966 | 424.1966 424.1996 | 4.46 7.07 | 248.1593, 230.1501, 105.0347, 91.0548 248.1601, 230.1490, 105.0316, 91.0541 | C ₂₁ H ₂₉ NO ₈ |  | 0.94 |

¹Estimated by ChemBio3D Ultra

Table 2: Postulated structures for MDPV and its Phase I and Phase II metabolites.

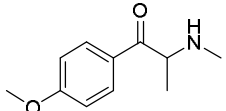
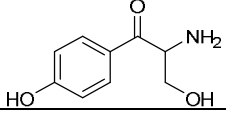
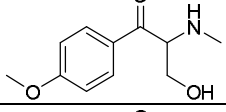
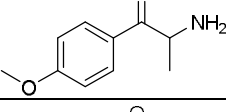
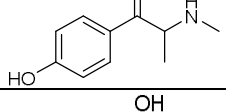
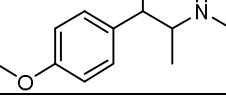
| Compound | Retention time (min) | Theoretical m/z $[M+H]^+$ | Measured m/z $[M+H]^+$ | Error (ppm) | Diagnostic product ions | Chemical formula | Structure | logKow ¹ |
|-------------|----------------------|-----------------------------|--------------------------|-------------|---|---|---|---------------------|
| MDPV | 19.17 | 276.1594 | 276.1594 | 0.00 | 205.0866, 175.0762, 149.0242, 135.0448, 126.1289, 84.0821 | C ₁₆ H ₂₁ NO ₃ |  | 3.06 |
| M1 | 12.56 | 280.1543 | 280.1544 | 0.36 | 262.1458, 191.0703, 139.0390, 109.0283, 72.0813 | C ₁₅ H ₂₁ NO ₄ |  | 1.70 |
| M2 | 13.21 | 264.1599 | 264.1605 | 2.27 | 175.0762, 137.0246, 126.1291, 123.0454, 109.0302 | C ₁₅ H ₂₁ NO ₃ |  | 2.92 |
| M3 | 14.20 | 262.1438 | 262.1439 | 0.38 | 220.0987, 178.0514, 145.0662, 127.0547 | C ₁₅ H ₁₉ NO ₃ |  | 2.49 |
| M4 | 16.15 | 310.1649 | 310.1636 | -4.19 | 292.1556, 274.1461, 246.1493, 175.0736, 149.0243, 71.0498 | C ₁₆ H ₂₃ NO ₅ |  | 1.14 |
| M5 | 16.25 | 222.1125 | 222.1112 | -5.85 | 204.1002, 174.0900, 146.0941, 117.0552, 135.0426 | C ₁₂ H ₁₅ NO ₃ |  | 1.94 |
| M6 | 16.79 | 260.1281 | 260.1272 | -3.46 | 230.0812, 202.0851, 156.0799 | C ₁₅ H ₁₇ NO ₃ |  | 3.00 |
| M7 | 17.14 | 292.1543 | 292.1547 | 1.37 | 274.1467, 205.0853, 149.0243, 142.1233, 135.0454, 121.0299, 70.0670 | C ₁₆ H ₂₁ NO ₄ |  | 2.53, 2.05 |

| | | | | | | | | |
|----------------------|-------|----------|----------|-------|--|---|---|------|
| M8 | 17.49 | 294.1700 | 294.1697 | -1.02 | 276.1583, 258.1461, 246.1491, 204.1012, 174.0815, 149.0236, 135.0439 | C ₁₆ H ₂₃ NO ₄ |  | 1.55 |
| M9 | 17.86 | 308.1498 | 308.1495 | -0.97 | 290.1397, 272.1275, 260.1279, 214.1227, 187.0758, 149.0234, 135.0441, 140.1073 | C ₁₆ H ₂₁ NO ₅ |  | 1.31 |
| M10 | 18.61 | 278.1751 | 278.1733 | -6.47 | 260.1678, 217.1126 | C ₁₆ H ₂₃ NO ₃ |  | 2.76 |
| M2-GLUa | 9.55 | 440.1915 | 440.1921 | 1.36 | 264.1611, 193.0878, 126.1307, 72.0835 | C ₂₁ H ₂₉ NO ₉ |  | 0.95 |
| M2-GLUb | 11.21 | | 440.1938 | 5.22 | 264.1588, 193.0863, 126.1288, 72.0829 | | | |
| M2-SULa ² | 13.42 | 342.1017 | 342.1003 | -4.09 | 262.1460, 193.0826, 163.0409, 136.0158, 108.0214 | C ₁₅ H ₂₁ NO ₆ S |  | 1.40 |
| M2-SULb ² | 14.21 | | 342.1017 | 0.00 | 262.1457, 193.0397, 136.0155, 108.0219 | | | |
| M3-GLUa | 8.73 | 438.1759 | 438.1766 | 1.60 | 262.1440, 234.1491 | C ₂₁ H ₂₇ NO ₉ |  | 0.53 |
| M3-GLUb | 9.41 | | 438.1758 | -0.23 | 262.1459, 234.1518 | | | |
| M6-GLUa | 13.46 | 436.1602 | 436.1590 | -2.75 | 260.1307 | C ₂₁ H ₂₅ NO ₉ |  | 1.04 |
| M6-GLUb | 14.35 | | 436.1616 | 3.21 | 260.1284 | | | |

¹Estimated by ChemBio3D Ultra

²Data in negative mode

Table 3: Postulated structures for methedrone and its Phase I metabolites.

| Compound | Retention time (min) | Theoretical m/z [M+H] ⁺ | Measured m/z [M+H] ⁺ | Error (ppm) | Diagnostic product ions | Chemical formula | Structure | logKow ¹ |
|-------------------|----------------------|--------------------------------------|-----------------------------------|-------------|--|---|--|---------------------|
| Methedrone | 18.71 | 194.1181 | 194.1190 | 4.64 | 176.1072, 161.0835, 146.0602, 132.0809, 118.0654, 103.0530, 91.0552, 77.0397 | C ₁₁ H ₁₅ NO ₂ |  | 1.58 |
| M1 | 7.27 | 182.0812 | 182.0816 | 2.20 | 165.0560, 147.0439, 136.0772, 123.0447, 107.0509, 91.0553, 77.0396 | C ₉ H ₁₁ NO ₃ |  | -0.24 |
| M2 | 8.94 | 210.1130 | 210.1121 | -4.28 | - | C ₁₁ H ₁₅ NO ₃ |  | 0.45 |
| M3 | 12.95 | 180.1024 | 180.1018 | -3.33 | 162.0905, 147.0682, 132.0466, 121.0639, 117.0575, 103.0561, 91.0550, 77.0390 | C ₁₀ H ₁₃ NO ₂ |  | 1.20 |
| M4 | 17.48 | 180.1024 | 180.1023 | -0.56 | 162.0906, 147.0673, 132.0431, 118.0656, 104.0491, 91.0543, 77.0391 | C ₁₀ H ₁₃ NO ₂ |  | 1.27 |
| M5 | 18.27 | 196.1337 | 196.1341 | 2.04 | 178.1226, 146.0964 | C ₁₁ H ₁₇ NO ₂ |  | 1.29 |

¹Estimated by ChemBio3D Ultra; - not data

Figure 1

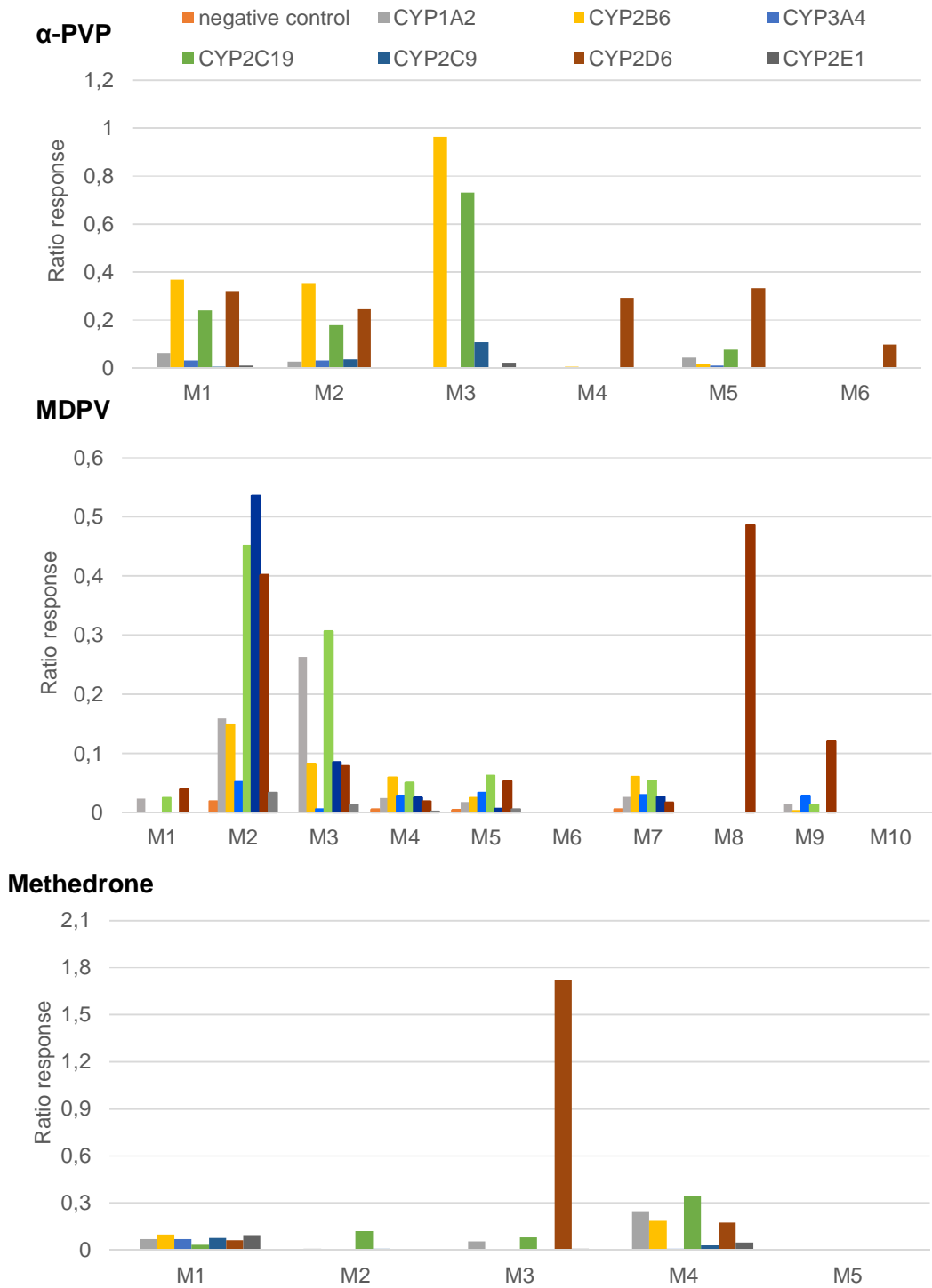


Figure 2

